Simulation of ADRC Application in Radio-Frequency Cavity

Presenter： Xue Yang

Advisor： Junqiang Zhang、Lingxi Ye、 Zhongquan Li

Affiliation： Chongqing University（LUTF）

目录 CONTENTS

Part I: Research Background

UTEF (Ultrafast Transient Experimental Facility)

Parameters	Value	Unit
Energy	0.5	GeV
Ring circumference	76.78	m
Beam current	0.5~1	A
Focusing type	QBA	
Natural emittance	8.56	nm rad
Working point (x, y)	6.198, 3.357	-
Length of straight section	8*4	m
Working frequency	499.8	MHz
Energy loss per turn	4.34	keV
Natural energy spread	0.37×10^{-3}	

Including the linac accelerator and the storage ring, with the storage ring operating at an energy of 0.5 GeV / 3 GeV.

Part I: Research Background

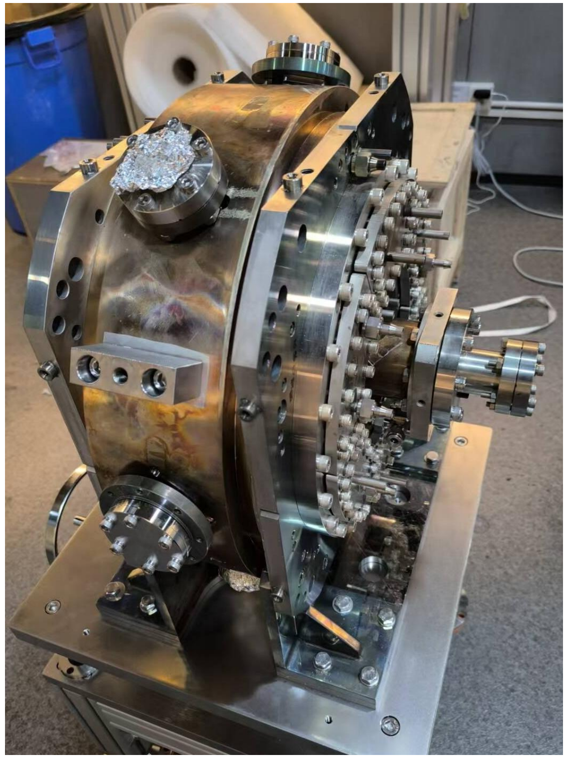

third-harmonic cavity

NC cavity with TM020 mode,
the first used in China

Frequency**: 1500 MHz** Q0:~**33000**

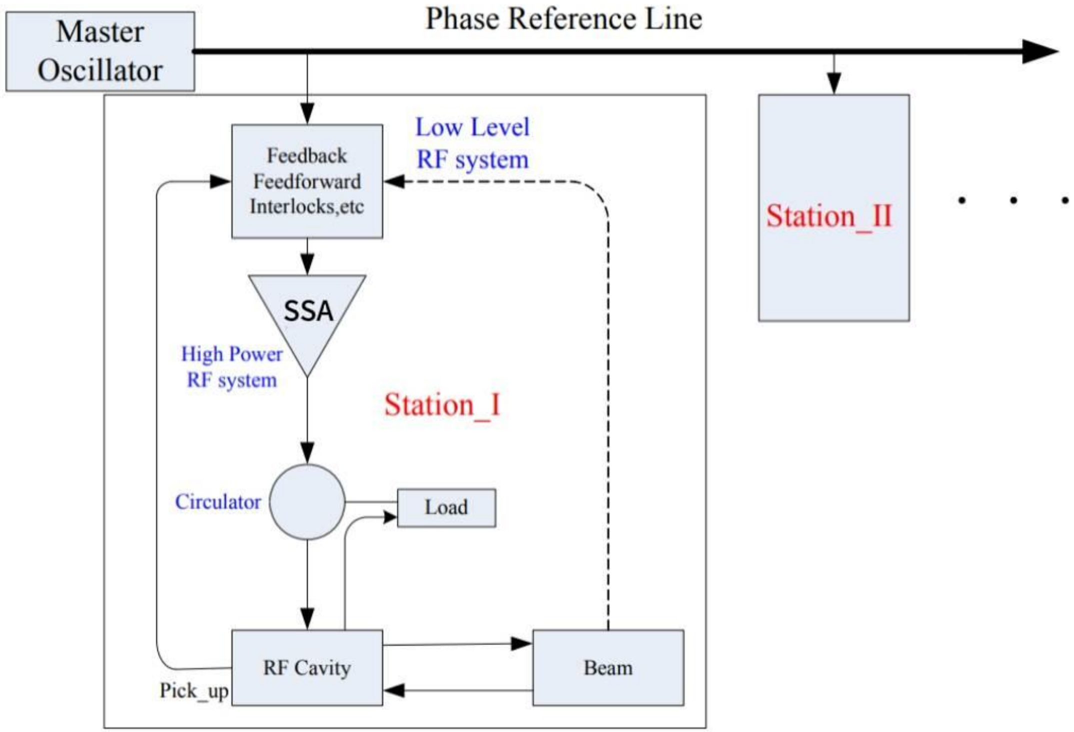

Low-Level Radio Frequency Systems

ADRC

Active Disturbance Rejection Control (ADRC) was first proposed in 1998 by Han Jingqing. It is a control algorithm independent of the plant model, **has huge potential in engineering applications.**

Extended State Observer (ESO) and State Error Feedback (SEF) :

ESO estimates $\hat{x}_1 \approx y$、$\hat{x}_2 \approx f$; SEF cancels the estimated disturbance $\hat{x}_2$ through feedforward and adds a proportional term $\ell(r-\hat{x}_1)$

$$\begin{aligned} \dot{\hat{x}}_1 &= \beta_1(y-\hat{x}_1) + l(r-\hat{x}_1) \\ \dot{\hat{x}}_2 &= \beta_2(y-\hat{x}_1) \\ u &= \frac{\ell(r-\hat{x}_1)-\hat{x}_2}{b_0} \end{aligned} \quad (1)$$

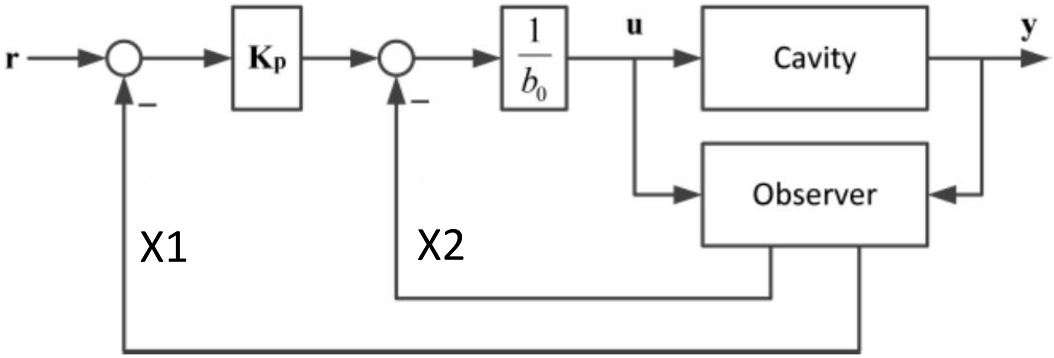

ADRC Framework Diagram

Laplace Transform

$$s\hat{X}_1(s) = -(\beta_1 + l)\hat{X}_1(s) + \beta_1 Y(s) + lR(s)$$
$$s\hat{X}_2(s) = -\beta_2\hat{X}_1(s) + \beta_2 Y(s)$$

$$\hat{X}_1 = \frac{\beta_1}{s+\beta_1+\ell}Y + \frac{\ell}{s+\beta_1+\ell}R$$

$$\hat{X}_2 = \frac{\beta_2}{s}(Y - \hat{X}_1)$$

$$U = \frac{\ell(R-\hat{X}_1) - \hat{X}_2}{b_0} = \frac{1}{b_0}\left[\ell R - \ell\hat{X}_1 - \frac{\beta_2}{s}(Y-\hat{X}_1)\right]$$

$$\frac{U(s)}{R(s)} == \boxed{\frac{\ell\,(s^2+\beta_1 s+\beta_2)}{b_0\, s\,(s+\beta_1+\ell)}}$$

$$\frac{U(s)}{Y(s)} == \boxed{-\frac{(\beta_1\ell+\beta_2)s+\beta_2\ell}{b_0\, s\,(s+\beta_1+\ell)}}$$

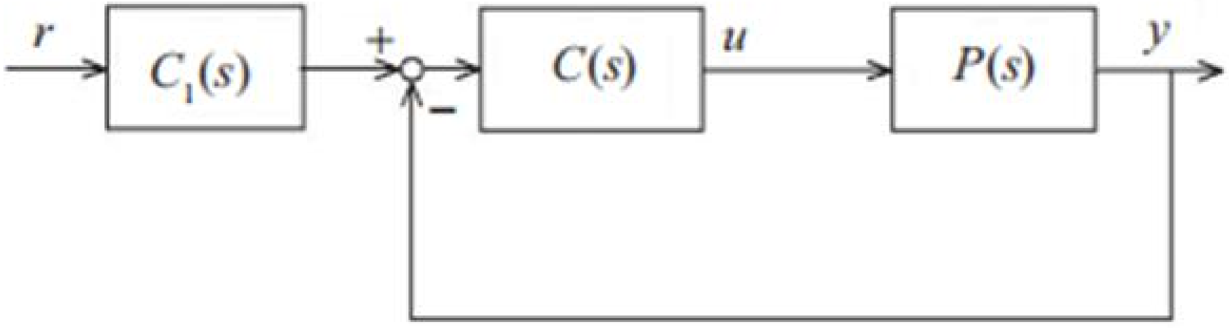

$$U(s) = C(s)(C_1(s)\,R(s) - Y(s))$$

$$\boxed{C(s) = -\frac{U(s)}{Y(s)} = \frac{(\beta_1\ell+\beta_2)s+\beta_2\ell}{b_0\, s\,(s+\beta_1+\ell)}}$$

$$\boxed{C_1(s) = \frac{U(s)/R(s)}{C(s)} = \frac{\ell\,(s^2+\beta_1 s+\beta_2)}{(\beta_1\ell+\beta_2)s+\beta_2\ell}}$$

Part II: Comparative Study of ADRC and PI Theory

$$C(s) = \frac{(\beta_1\ell + \beta_2)s + \beta_2\ell}{b_0\, s\,(s + \beta_1 + \ell)}$$

$$C(s) = \frac{\beta_1\ell + \beta_2}{b_0\,(+\beta_1 + \ell)} + \frac{\beta_2\ell}{b_0\, s\,(s + \beta_1 + \ell)}$$

$$= \frac{\beta_1 + \ell}{s + \beta_1 + \ell}\left[\frac{\beta_1\ell + \beta_2}{b_0(\beta_1 + \ell)} + \frac{\beta_2\ell}{b_0(\beta_1 + \ell)}\frac{1}{s}\right]$$

$$F(s) = \frac{\beta_1 + \ell}{s + \beta_1 + \ell} \qquad k_p = \frac{\beta_1\ell + \beta_2}{b_0(\beta_1 + \ell)} \qquad k_i = \frac{\beta_2\ell}{b_0(\beta_1 + \ell)}$$

$$C(s) = F(s)\left(k_p + \frac{k_i}{s}\right) = F(s) \cdot \mathrm{PI}(s)$$

Physical Significance: Here, $F(s)$ denotes a low-pass filter, while k_p and k_i represent the control parameters of the PI controller. Thus, the distinction between $C(s)$ and $PI(s)$ depends on the low-pass filter $F(s)$. When $\omega \gg \omega_F$, $C(s)$ exhibits superior noise suppression compared to $PI(s)$.

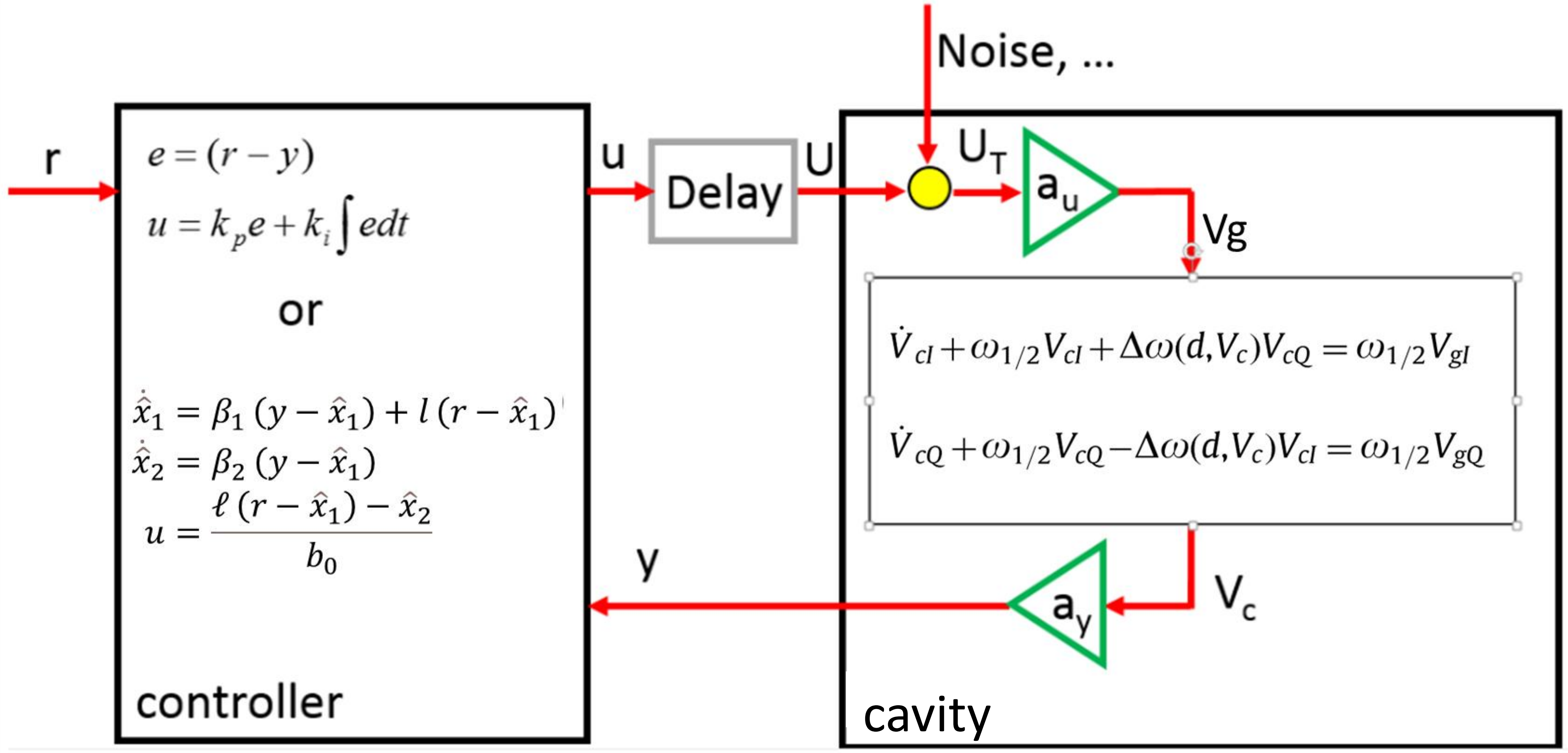

Block diagram of a LLRF system simulation model.

Part III: Simulation Analysis

重庆大学 CHONGQING UNIVERSITY

ESO State Matrix: $\begin{bmatrix}\dot{x}_1\\ \dot{x}_2\end{bmatrix} = \begin{bmatrix}0 & 1\\ 0 & 0\end{bmatrix}\begin{bmatrix}x_1\\ x_2\end{bmatrix} + \begin{bmatrix}0\\ b\end{bmatrix} u + \begin{bmatrix}\beta_1\\ \beta_2\end{bmatrix}(y - \hat{y})$

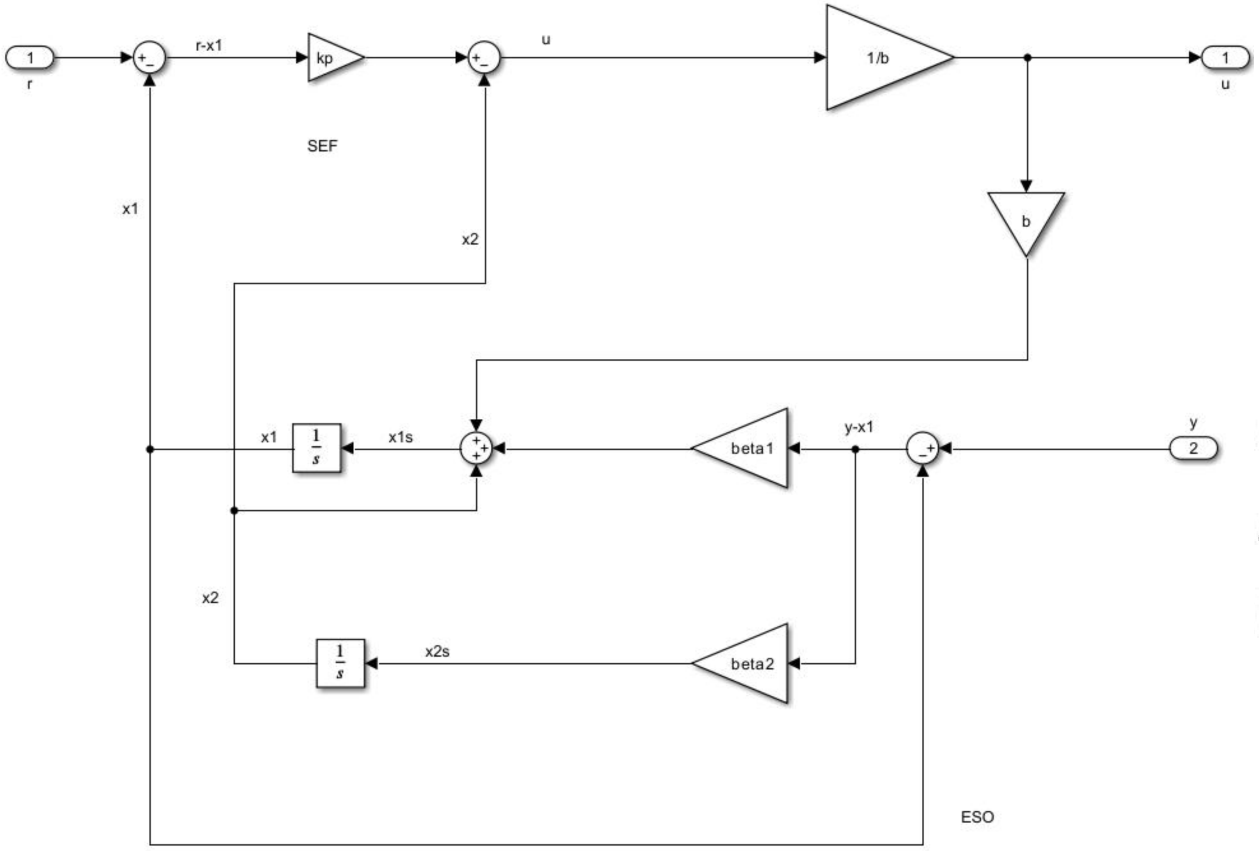

Framework Diagram of ADRC in Simulink

SEL: $u_0 = k_p(r - x_1)$

$\beta_1 = 2\omega_{ob}$

$\beta_2 = \omega_{ob}^2$

$k_p = \omega_c$

Part III: Simulation Analysis

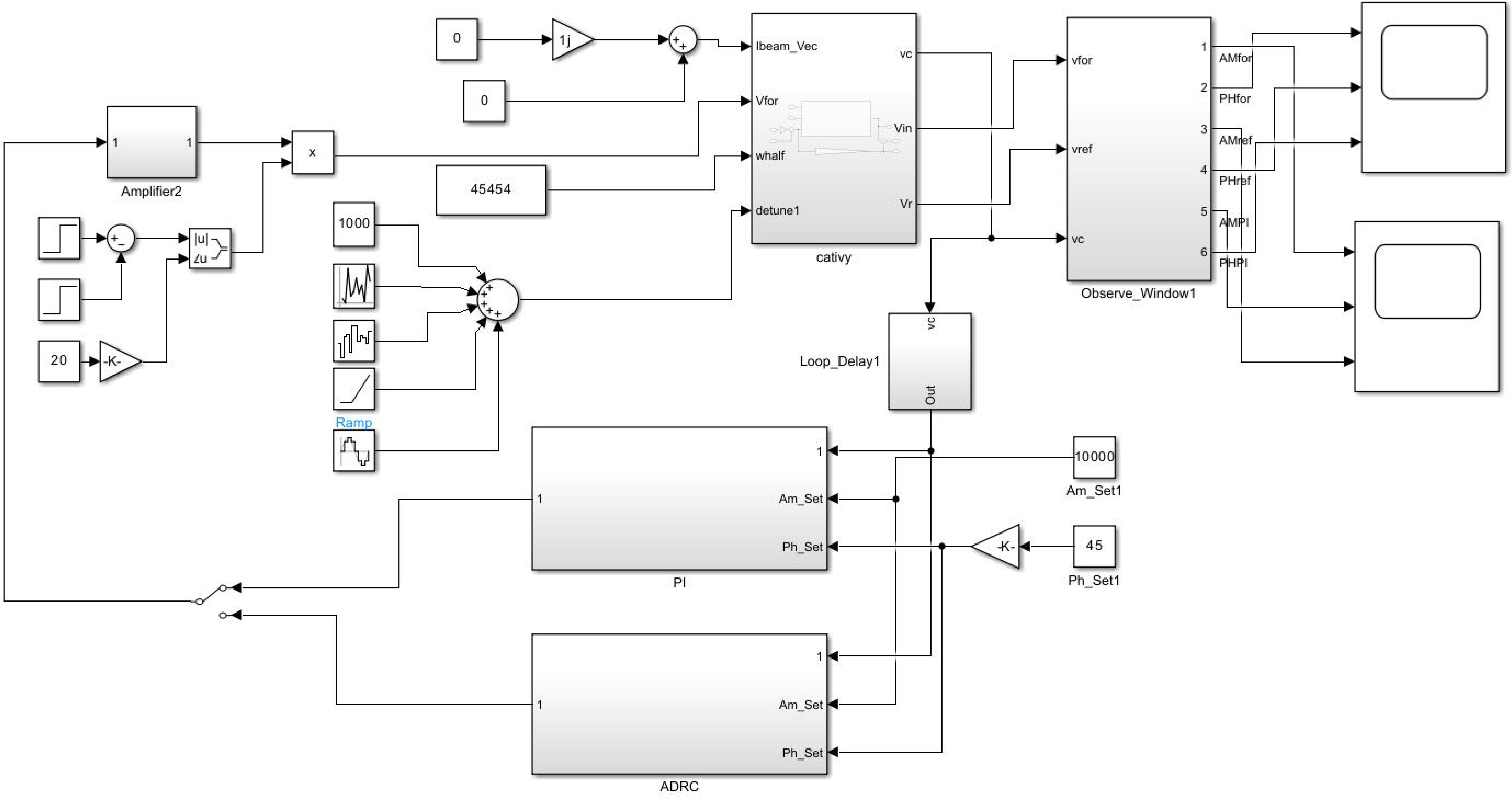

LLRF system simulation model

Part III: Simulation Analysis

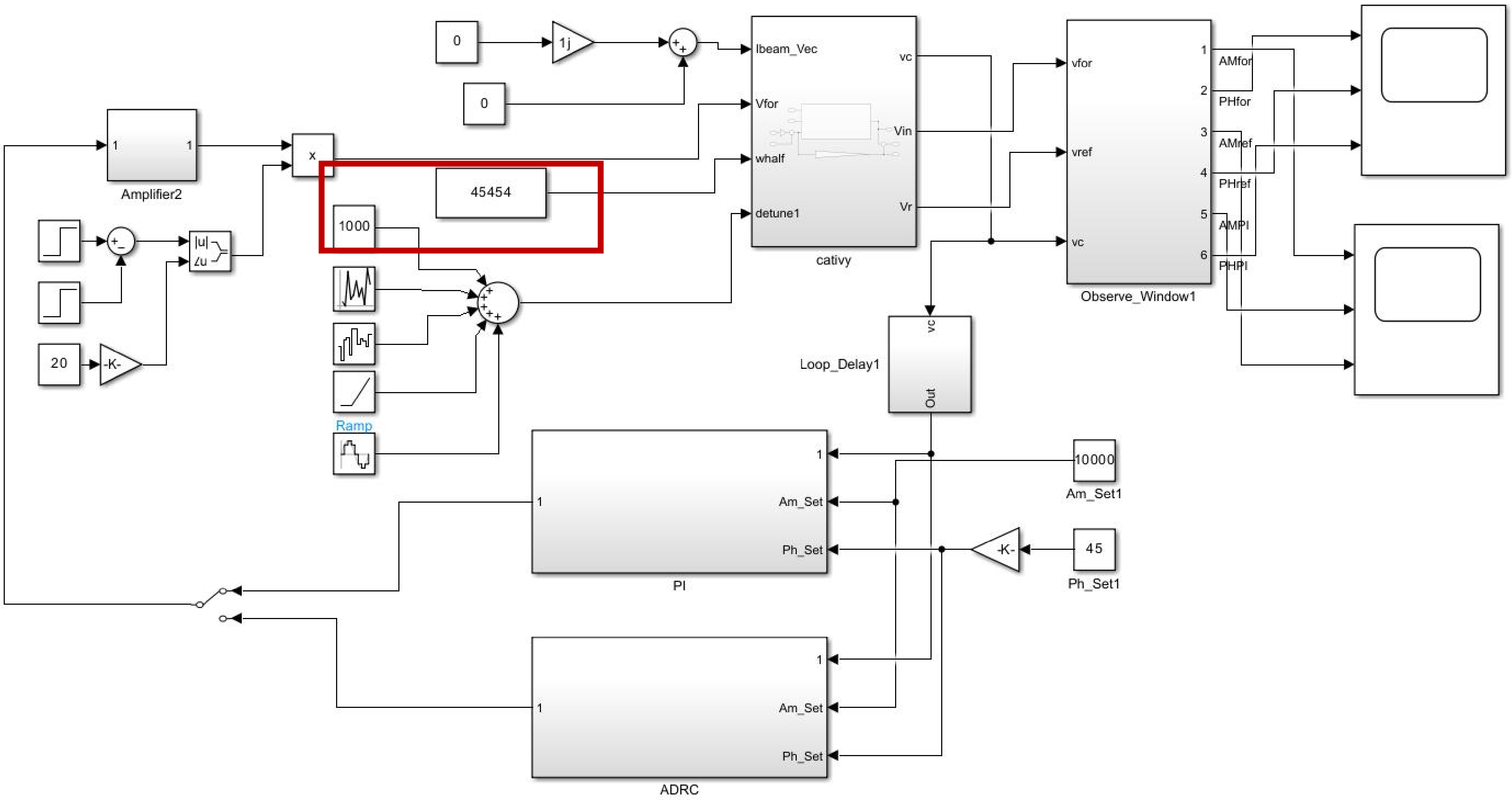

LLRF system simulation model

Part III: Simulation Analysis

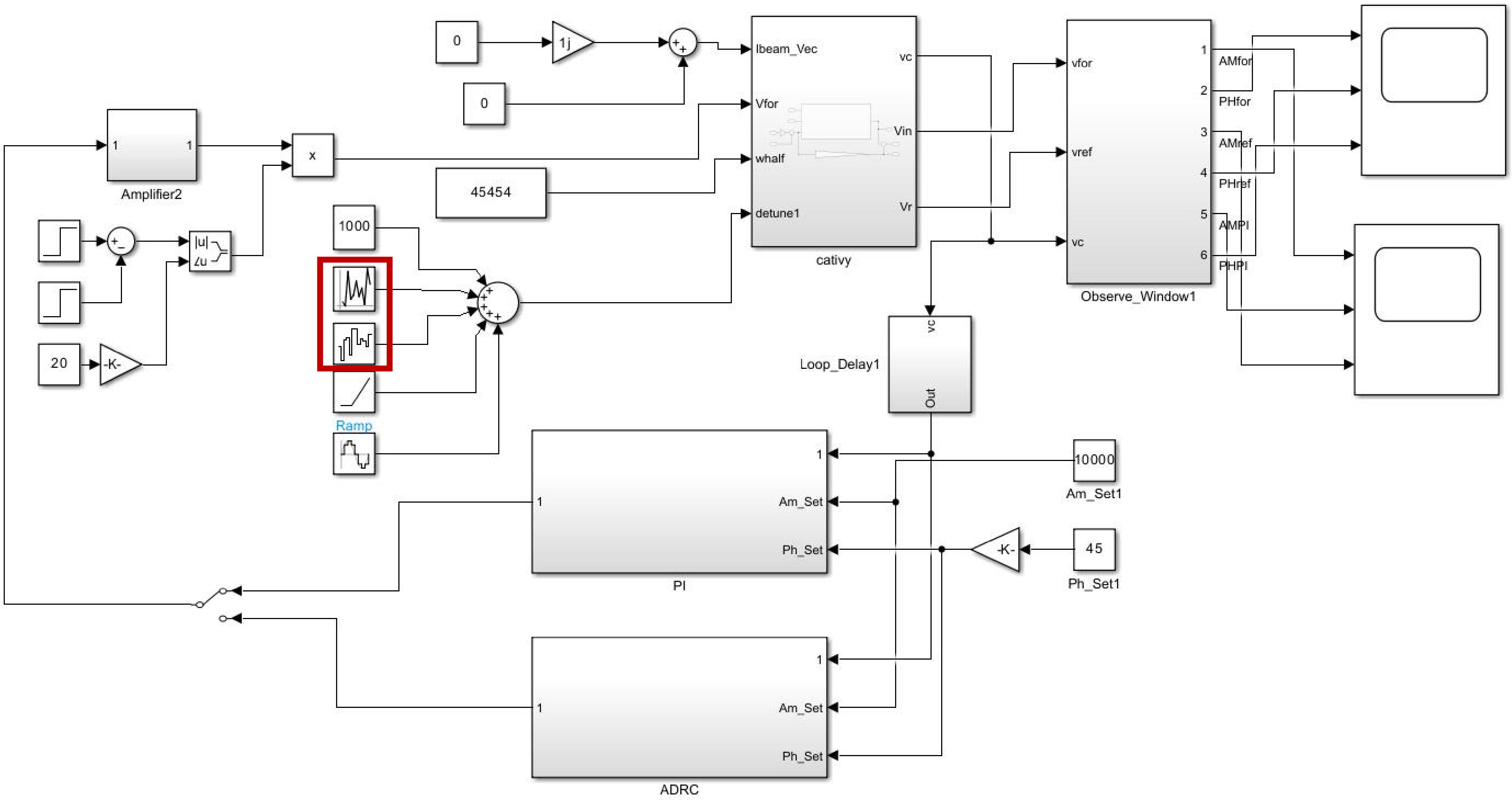

LLRF system simulation model

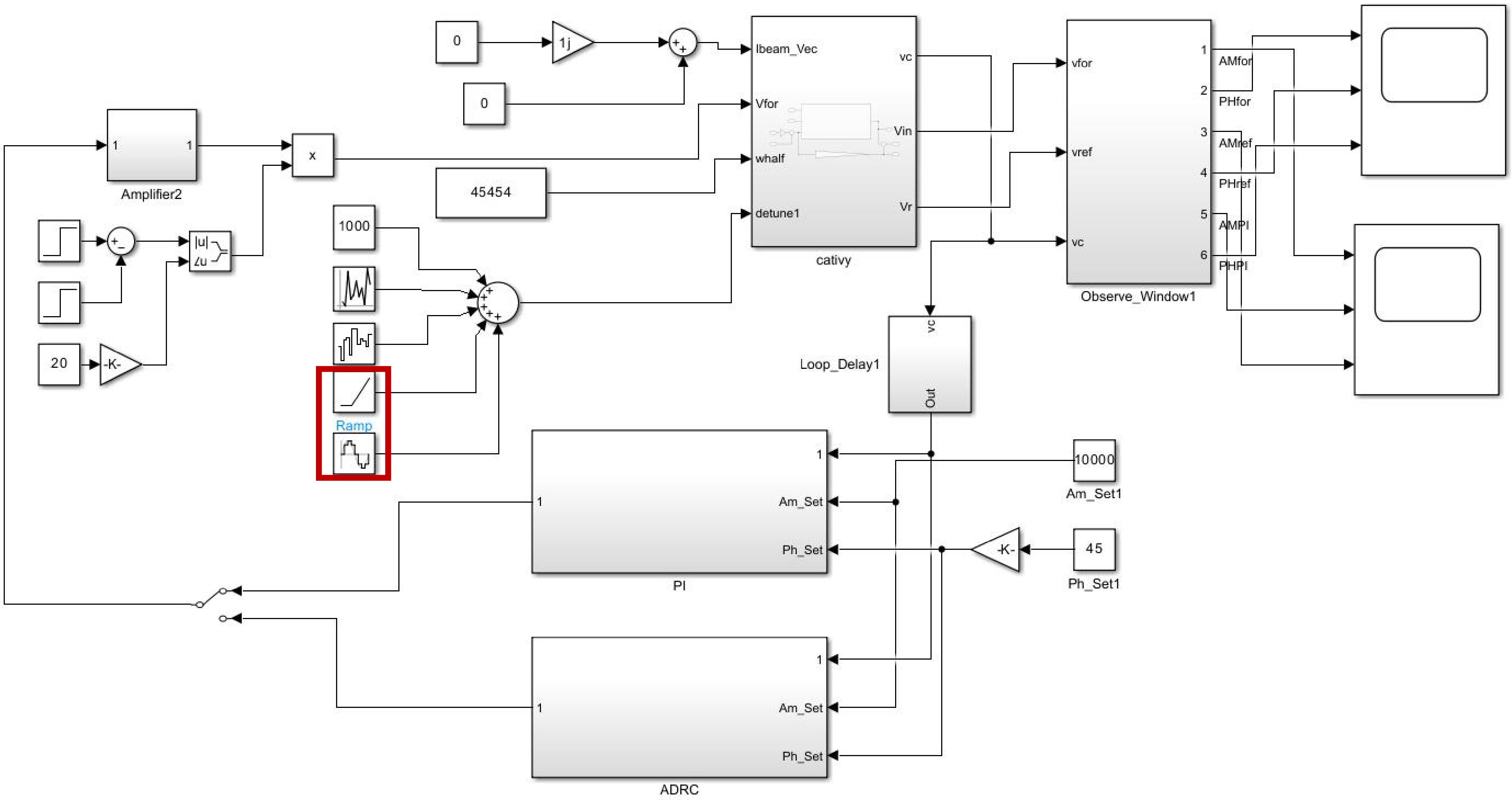

LLRF system simulation model

Cavity Response:

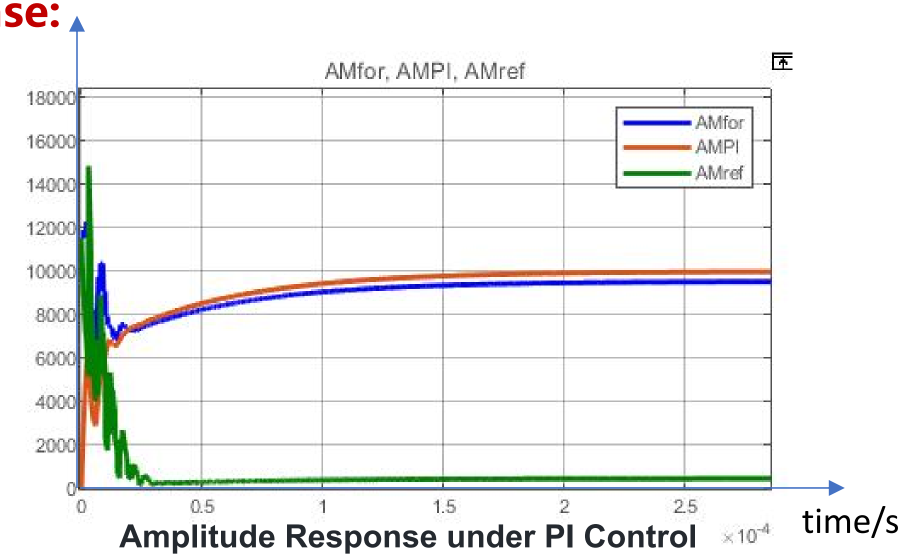

Amplitude Response under PI Control

Phase Response under PI Control

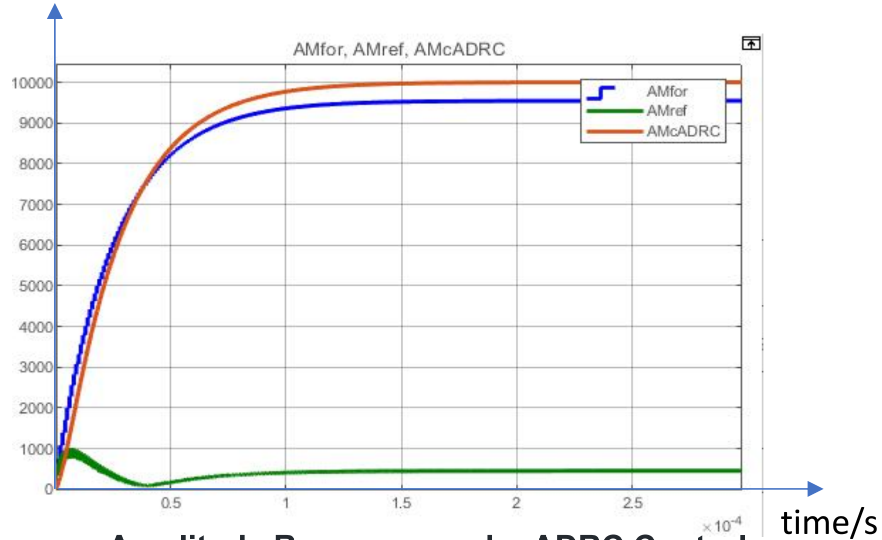

Amplitude Response under ADRC Control

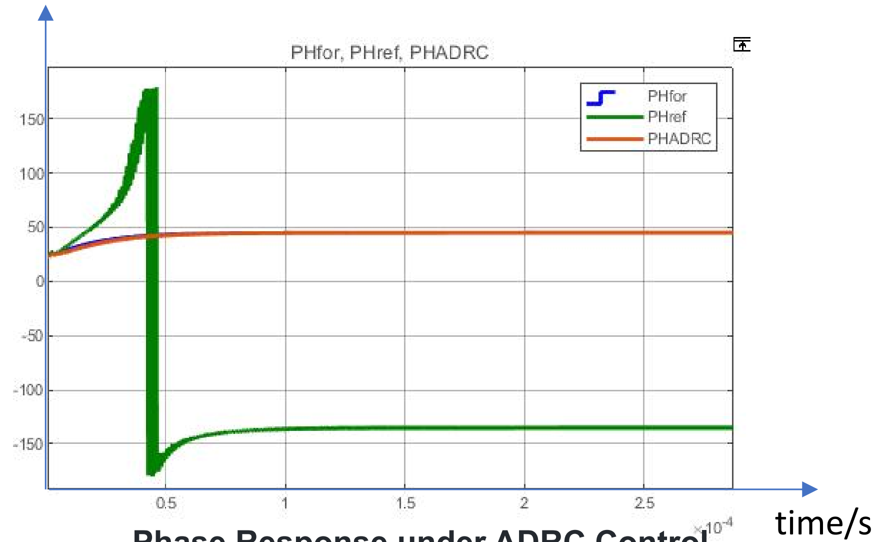

Phase Response under ADRC Control

Part III: Simulation Analysis

Detuning

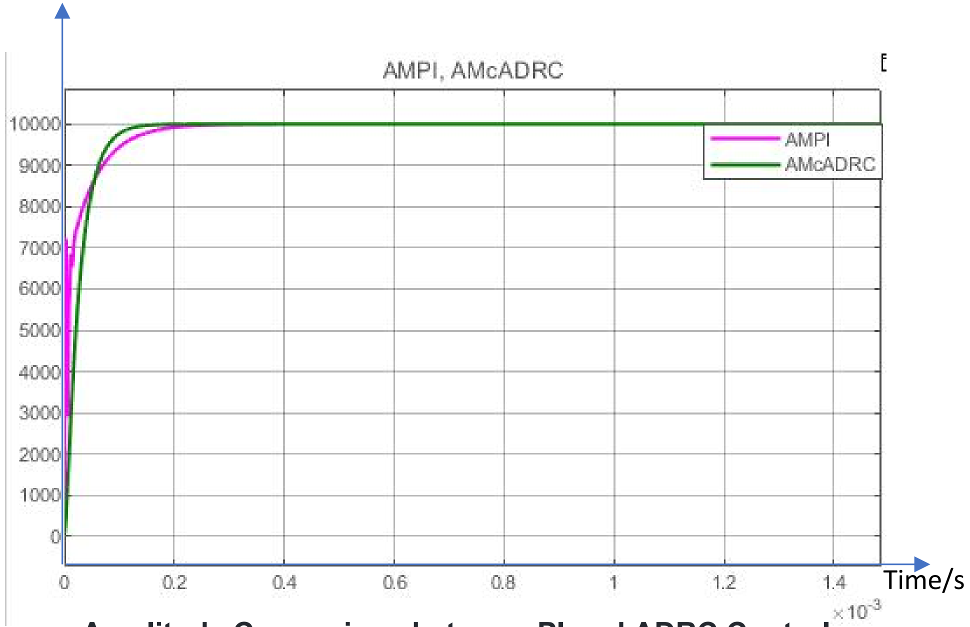

Amplitude Comparison between PI and ADRC Control

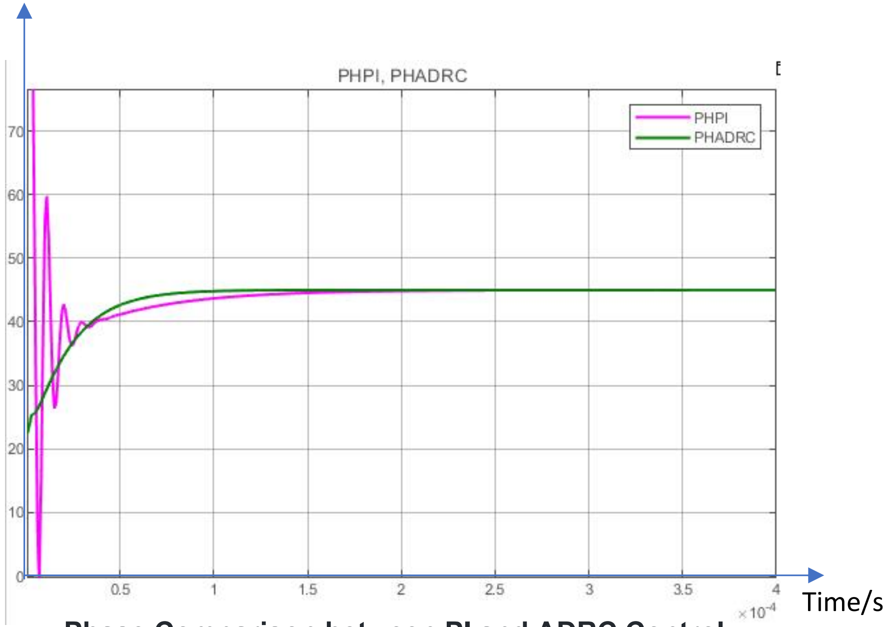

Phase Comparison between PI and ADRC Control

Part III: Simulation Analysis

Noise + Detuning

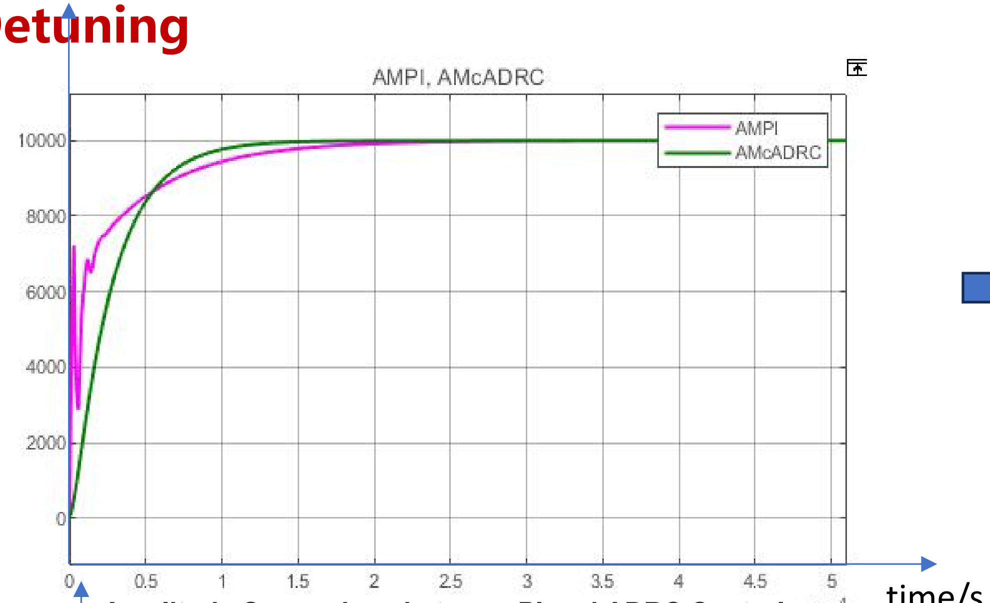

Amplitude Comparison between PI and ADRC Control

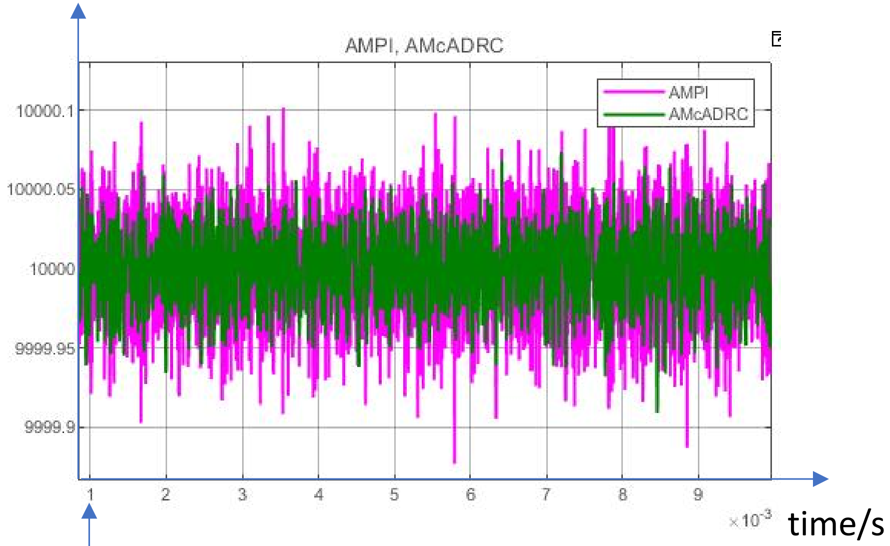

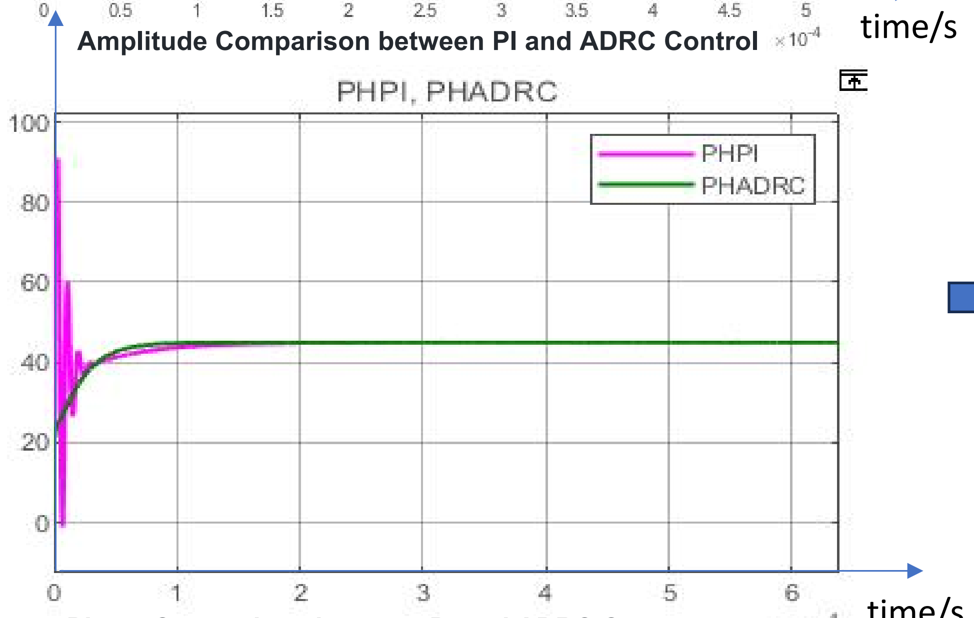

Phase Comparison between PI and ADRC Control

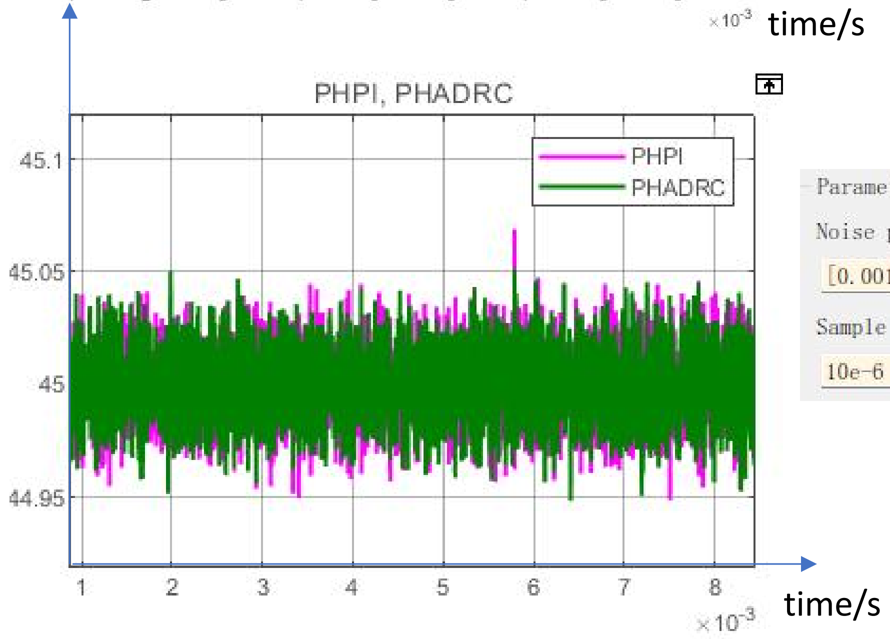

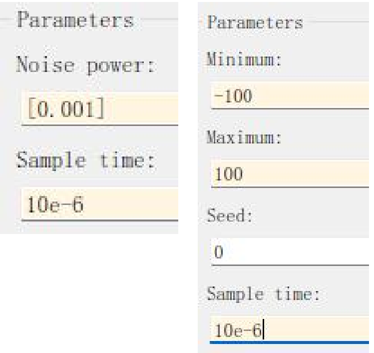

Part III: Simulation Analysis

The Influence of Temperature Drift

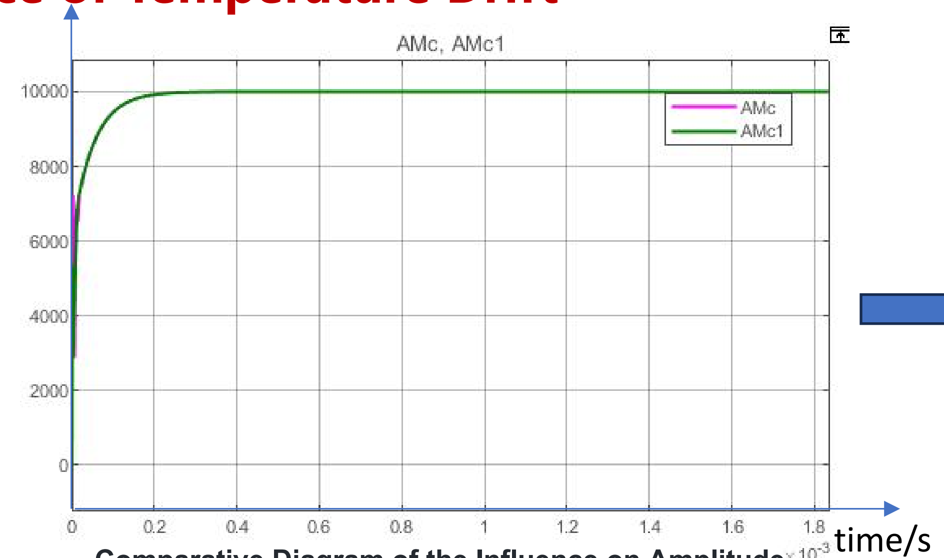

Comparative Diagram of the Influence on Amplitude

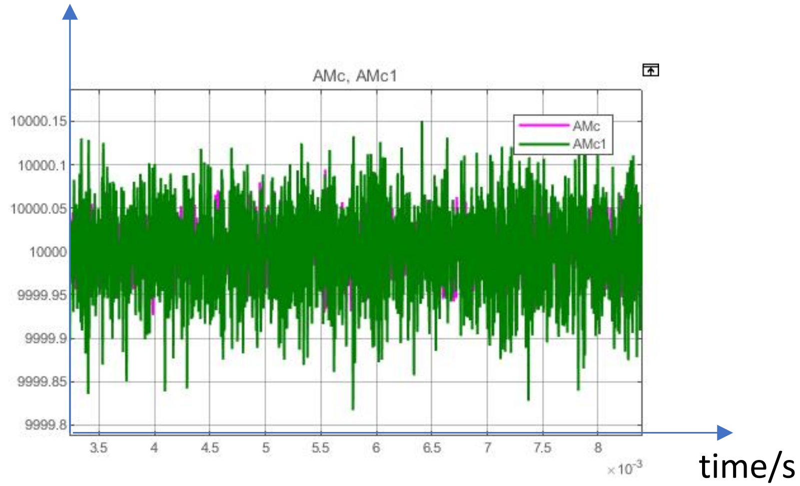

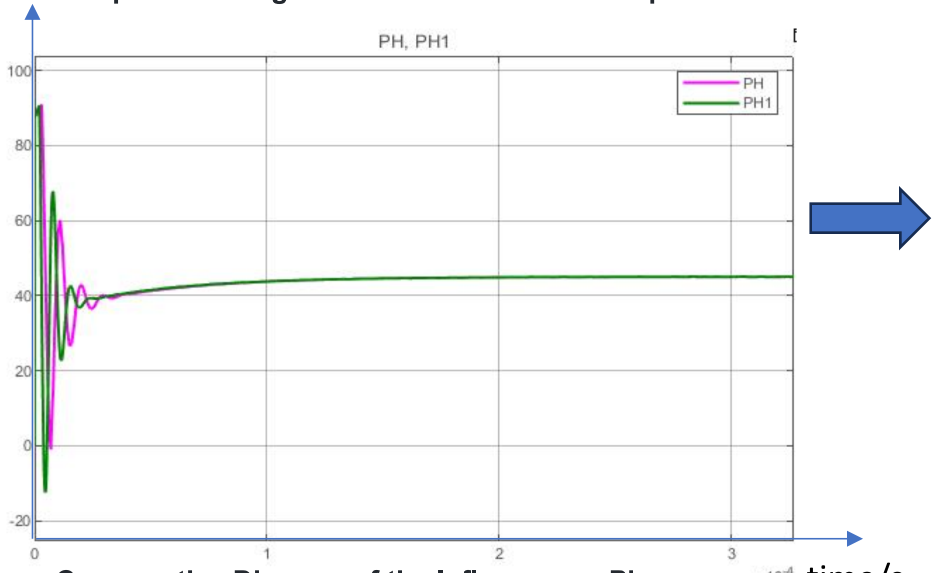

Comparative Diagram of the Influence on Phase

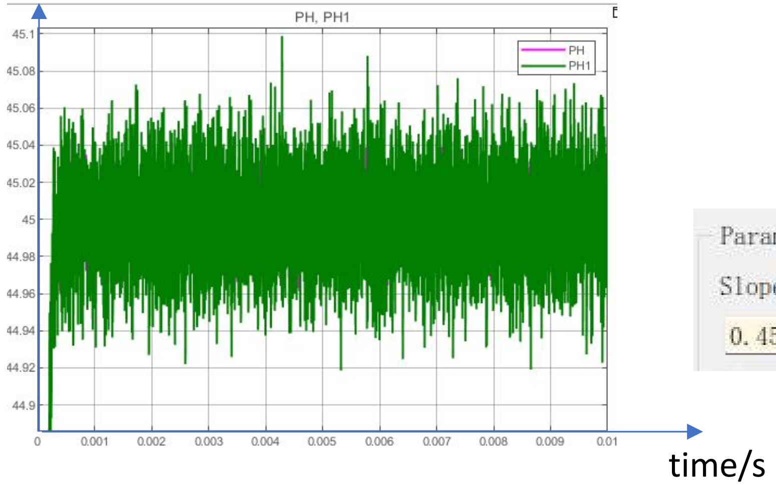

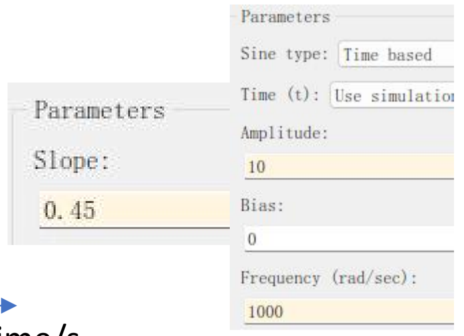

Part III: Simulation Analysis

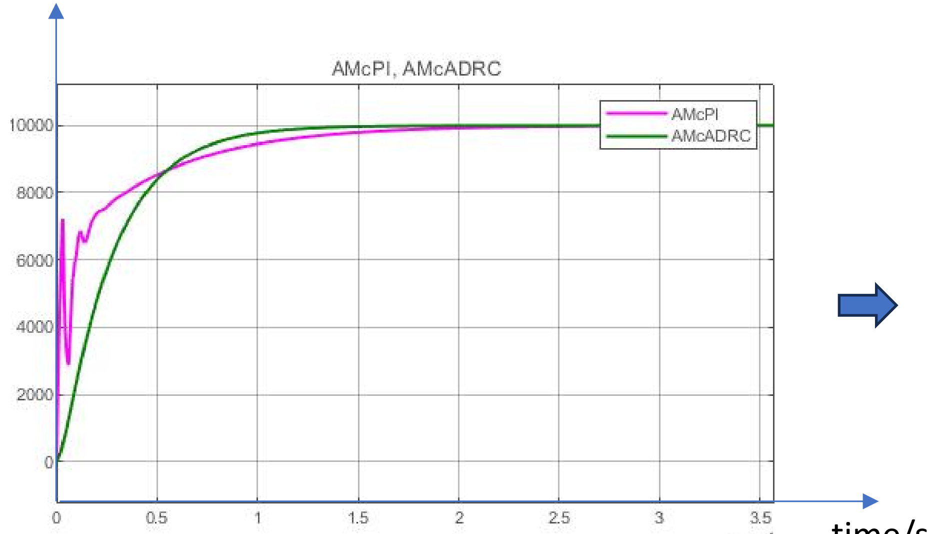

Amplitude Comparison between PI and ADRC Control

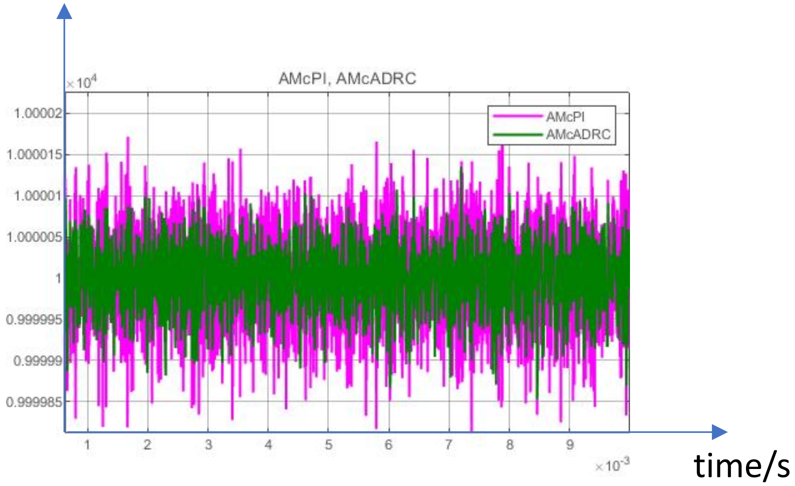

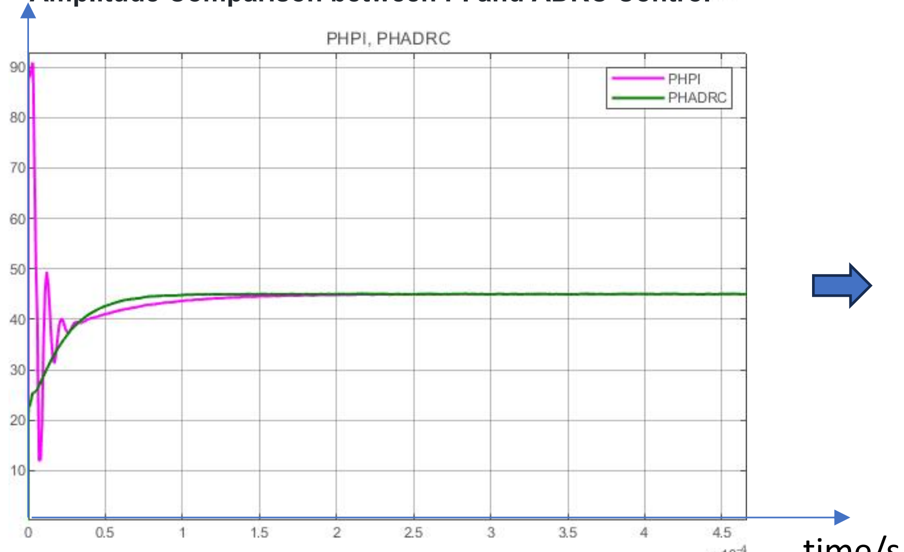

Phase Comparison between PI and ADRC Control

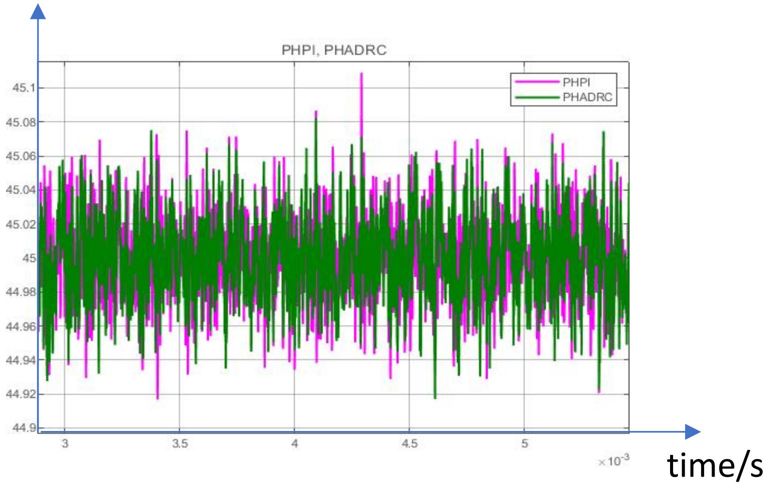

Part IV: Conclusion

Sammary ：

- According to the simulation results, ADRC demonstrates superior disturbance rejection performance compared to PI control.
- However, parameter tuning for ADRC is relatively complex.
- Next step： It is planned to implement ADRC assisted by PI in the LLRF systems of UTEF’s linac accelerator and storage ring to achieve better disturbance rejection.


Thank you!